Strangeness Suppression of $q\bar{q}$ Creation Observed in Exclusive Reactions

M. D. Mestayer,[32,*] K. Park,[32,†] K. P. Adhikari,[26] M. Aghasyan,[15] S. Anefalos Pereira,[15] J. Ball,[6] M. Battaglieri,[16]
V. Batourine,[32] I. Bedlinskiy,[19] A. S. Biselli,[9,4] S. Boiarinov,[32] W. J. Briscoe,[12] W. K. Brooks,[33,32] V. D. Burkert,[32]
D. S. Carman,[32] A. Celentano,[16] S. Chandavar,[25] G. Charles,[18] L. Colaneri,[29,17] P. L. Cole,[13,32] M. Contalbrigo,[14]
O. Cortes,[13] V. Crede,[11] A. D'Angelo,[17,29] N. Dashyan,[38] R. De Vita,[16] A. Deur,[32] C. Djalali,[31] D. Doughty,[7,32] R. Dupre,[18]
A. El Alaoui,[1,‡] L. El Fassi,[26] L. Elouadrhiri,[32] P. Eugenio,[11] G. Fedotov,[31,30] J. A. Fleming,[34] T. A. Forest,[13] B. Garillon,[18]
M. Garçon,[6] Y. Ghandilyan,[38] G. P. Gilfoyle,[28] K. L. Giovanetti,[20] F. X. Girod,[32] J. T. Goetz,[25] E. Golovatch,[30]
R. W. Gothe,[31] K. A. Griffioen,[37] B. Guegan,[18] M. Guidal,[18] H. Hakobyan,[33,38] C. Hanretty,[36,§] M. Hattawy,[18] M. Holtrop,[23]
S. M. Hughes,[34] C. E. Hyde,[26] Y. Ilieva,[31,12] D. G. Ireland,[35] H. Jiang,[31] H. S. Jo,[18] K. Joo,[8] D. Keller,[36] M. Khandaker,[13,24]
A. Kim,[21,‖] W. Kim,[21] S. Koirala,[26] V. Kubarovsky,[32,27] S. V. Kuleshov,[33,19] P. Lenisa,[14] W. I. Levine,[4] K. Livingston,[35]
H. Y. Lu,[31] I. J. D. MacGregor,[35] M. Mayer,[26] B. McKinnon,[35] C. A. Meyer,[4] M. Mirazita,[15] V. Mokeev,[32,30]
R. A. Montgomery,[15,¶] C. I. Moody,[1] H. Moutarde,[6] A. Movsisyan,[14] C. Munoz Camacho,[18] P. Nadel-Turonski,[32]
S. Niccolai,[18,12] G. Niculescu,[20,25] I. Niculescu,[20] M. Osipenko,[16] A. I. Ostrovidov,[11] L. L. Pappalardo,[14] R. Paremuzyan,[38,**]
P. Peng,[36] W. Phelps,[10] S. Pisano,[15] O. Pogorelko,[19] S. Pozdniakov,[19] J. W. Price,[27,3] D. Protopopescu,[35] A. J. R. Puckett,[8]
B. A. Raue,[10,32] D. Rimal,[10] M. Ripani,[16] A. Rizzo,[17] G. Rosner,[35] P. Roy,[11] F. Sabatié,[6] M. S. Saini,[11] D. Schott,[12]
R. A. Schumacher,[4] A. Simonyan,[38] D. Sokhan,[35] S. Strauch,[31,12] V. Sytnik,[33] W. Tang,[25] Ye Tian,[31] M. Ungaro,[32,27]
B. Vernarsky,[4] A. V. Vlassov,[19] H. Voskanyan,[38] E. Voutier,[22] N. K. Walford,[5] D. P. Watts,[34] X. Wei,[32] L. B. Weinstein,[26]
M. H. Wood,[2,31] N. Zachariou,[31] J. Zhang,[32] Z. W. Zhao,[36] and I. Zonta[17]

(CLAS Collaboration)

[1]*Argonne National Laboratory, Argonne, Illinois 60439, USA*
[2]*Canisius College, Buffalo, New York 14208, USA*
[3]*California State University, Dominguez Hills, Carson, California 90747, USA*
[4]*Carnegie Mellon University, Pittsburgh, Pennsylvania 15213, USA*
[5]*Catholic University of America, Washington, D.C. 20064, USA*
[6]*CEA, Centre de Saclay, Irfu/Service de Physique Nucléaire, 91191 Gif-sur-Yvette, France*
[7]*Christopher Newport University, Newport News, Virginia 23606, USA*
[8]*University of Connecticut, Storrs, Connecticut 06269, USA*
[9]*Fairfield University, Fairfield, Connecticut 06824, USA*
[10]*Florida International University, Miami, Florida 33199, USA*
[11]*Florida State University, Tallahassee, Florida 32306, USA*
[12]*The George Washington University, Washington, D.C. 20052, USA*
[13]*Idaho State University, Pocatello, Idaho 83209, USA*
[14]*INFN, Sezione di Ferrara, 44100 Ferrara, Italy*
[15]*INFN, Laboratori Nazionali di Frascati, 00044 Frascati, Italy*
[16]*INFN, Sezione di Genova, 16146 Genova, Italy*
[17]*INFN, Sezione di Roma Tor Vergata, 00133 Rome, Italy*
[18]*Institut de Physique Nucléaire ORSAY, Orsay, France*
[19]*Institute of Theoretical and Experimental Physics, Moscow 117259, Russia*
[20]*James Madison University, Harrisonburg, Virginia 22807, USA*
[21]*Kyungpook National University, Daegu 702-701, Republic of Korea*
[22]*LPSC, Université Grenoble-Alpes, CNRS/IN2P3, Grenoble, France*
[23]*University of New Hampshire, Durham, New Hampshire 03824-3568, USA*
[24]*Norfolk State University, Norfolk, Virginia 23504, USA*
[25]*Ohio University, Athens, Ohio 45701, USA*
[26]*Old Dominion University, Norfolk, Virginia 23529, USA*
[27]*Rensselaer Polytechnic Institute, Troy, New York 12180-3590, USA*
[28]*University of Richmond, Richmond, Virginia 23173, USA*
[29]*Universita' di Roma Tor Vergata, 00133 Rome, Italy*
[30]*Skobeltsyn Institute of Nuclear Physics, Lomonosov Moscow State University, 119234 Moscow, Russia*
[31]*University of South Carolina, Columbia, South Carolina 29208, USA*
[32]*Thomas Jefferson National Accelerator Facility, Newport News, Virginia 23606, USA*
[33]*Universidad Técnica Federico Santa María, Casilla 110-V Valparaíso, Chile*

[34]*Edinburgh University, Edinburgh EH9 3JZ, United Kingdom*
[35]*University of Glasgow, Glasgow G12 8QQ, United Kingdom*
[36]*University of Virginia, Charlottesville, Virginia 22901, USA*
[37]*College of William and Mary, Williamsburg, Virginia 23187-8795, USA*
[38]*Yerevan Physics Institute, 375036 Yerevan, Armenia*

We measured the ratios of electroproduction cross sections from a proton target for three exclusive meson-baryon final states: ΛK^+, $p\pi^0$, and $n\pi^+$, with the CLAS detector at Jefferson Lab. Using a simple model of quark hadronization, we extract $q\bar{q}$ creation probabilities for the first time in exclusive two-body production, in which only a single $q\bar{q}$ pair is created. We observe a sizable suppression of strange quark-antiquark pairs compared to nonstrange pairs, similar to that seen in high-energy production.

At high energies, the production of hadrons is well described by a model in which the color "flux tube" is "broken" by a series of $q\bar{q}$ pair creation events followed by a regrouping of the quarks and antiquarks into color singlet hadrons. The modeling of the strong force as a color flux tube explained the linear binding potential of heavy $q\bar{q}$ "quarkonia" states, while quark-pair creation models [1] developed in the 1970s accounted for hadronic production and the nonobservance of free quarks.

The "Lund model" [2] was formulated in the 1980s to quantify the fragmentation of very high-momentum quarks into "jets" of observed hadrons. The $q\bar{q}$ pair creation process is modeled as tunneling in a linear potential, resulting in a probability proportional to the exponential of the quark mass squared divided by the flux-tube tension of ≈ 1 GeV/fm. Calculations with plausible quark masses indicated that $s\bar{s}$ production is reduced by a factor of about one third relative to that for $u\bar{u}$ or $d\bar{d}$. This reduction factor is known as the "strangeness suppression factor" and is empirically adjusted to approximate the observed production rates of hadrons.

Strangeness suppression has been studied by various hadron-production experiments [3] resulting in a successful extension of the Lund model into, among others, the JETSET and PYTHIA event generators [4] which reproduce observed hadronic production rates in high energy reactions. Typically, a strangeness suppression factor, $\lambda_s \approx 0.3$ describes the data well in e^+e^- collisions up to center-of-mass energies of the Z boson mass [5] and in high-energy deep-inelastic electron proton scattering [6].

Although $q\bar{q}$ creation is the "kernel" of the process which transforms quarks into observable hadrons, it is not well understood. We designed our study to extract the flavor dependence of $q\bar{q}$ creation in a new kinematic region: the two-body exclusive limit in which a single $q\bar{q}$ pair is created, there are no decay chains to model and for which we can do an explicit phase-space correction.

In pseudoscalar-meson electroproduction, a beam of electrons is incident upon a proton target, producing a final state consisting of the scattered electron and the outgoing baryon and pseudoscalar meson. After integrating over the azimuthal angle of the scattered electron, the cross section can be expressed in terms of the variables Q^2, W, θ_m^*, and ϕ, where $q^2 = -Q^2$ is the squared four momentum of the virtual photon, W is the total hadronic energy in the center-of-mass frame, θ_m^* is the meson angle in the $\gamma^* p$ center-of-mass system, and ϕ is the azimuthal angle of the reaction plane with respect to the electron scattering plane.

The differential cross section can be expressed as:

$$\frac{d\sigma}{dQ^2 dW d\Omega_m^*} = \Gamma_v(\sigma_T + \epsilon\sigma_L + \epsilon\sigma_{TT}\cos 2\phi + \sqrt{\epsilon(\epsilon+1)}\sigma_{LT}\cos\phi), \quad (1)$$

where Γ_v is the flux of virtual photons, ϵ is the polarization parameter, and the four structure functions, σ_T, σ_L, σ_{TT}, and σ_{LT} are the transverse and longitudinal response functions and the two interference terms, respectively. This formalism is explained in more detail in a previous CLAS collaboration paper [7].

Our study was part of a larger program to measure electroproduction of hadrons from a proton target. The electron beam energy was 5.499 GeV, with a typical intensity of 7 nA, incident on a 5-cm liquid hydrogen target. The signal from the scattered electron provided the data-acquisition trigger. The data-taking period lasted for 42 days and resulted in the collection of ~4.3 billion events. After event reconstruction, ~650 million events remained with at least one good electron candidate.

The scattered electron and associated hadrons were measured in the CLAS detector, a large-acceptance magnetic spectrometer [8] based on a six-coil toroidal magnet with drift chambers providing charged particle tracking, followed by a Cherenkov detector for electron identification, and scintillators and an electromagnetic calorimeter for particle identification by time of flight and energy deposition, respectively.

The electron was identified by matching a negatively charged track in the drift chambers with signals in the Cherenkov counter and in the electromagnetic calorimeter. The identity of the positively charged particle candidate

TABLE I. Kinematic binning used in this analysis.

Quantity	Number Bin	Bin Limits
W (GeV)	6	1.65, 1.75, 1.85, 1.95, 2.05, 2.25, 2.55
Q^2 (GeV^2)	2	1.6, 2.6, 4.6
$\cos\theta_m^*$	5	$-1.0, -0.6, -0.2, 0.2, 0.6, 1.0$
ϕ (deg)	12	$-180, -150, \ldots 150, 180$

was determined by combining the flight time from the time-of-flight counters with the momentum and track length from the drift chamber track to calculate the particle's velocity (β) and mass.

We analyzed events with a final state consisting of the scattered electron plus one positively charged particle (a K^+, π^+, or proton). We measured the four momenta of the scattered electron and charged hadron, and determined by missing mass that the undetected neutral particle was a Λ, a neutron, or a π^0, respectively.

The scattered electron's and charged hadron's four momenta were used to calculate the independent kinematic variables: Q^2, W, $\cos\theta_m^*$, and ϕ. Our kinematic coverages are $W = 1.65$–2.55 GeV, $Q^2 = 1.6$–4.6 GeV^2 and the full range of $\cos\theta_m^*$ and ϕ. We defined 720 bins in this four-dimensional space (see Table I).

For each event, the missing-mass recoiling from the scattered electron and identified hadron was calculated and, by accumulating over all events, a missing-mass distribution was formed for each four-dimensional kinematic bin. For the $p\pi^0$ final state, an additional series of cuts was employed to remove radiative elastic-scattering events before our fits and mass cuts were applied. We then fit each missing-mass distribution to a function consisting of a Gaussian peak for the signal and a smooth polynomial for the background. We subtracted the background portion of the fit and counted the number of events within a fixed missing-mass range to obtain the raw yield, using the fit values for determination of the statistical uncertainty of the yield.

Corrections for finite acceptance and inefficiencies in track reconstruction, particle identification, and missing-mass cuts were made. A Monte Carlo simulation, tuned to match the momentum resolution of the detector, accounted for run-dependent inefficiencies due to malfunctioning subsystem components.

The acceptance-corrected yields were further corrected by a two-body phase-space factor [9],

$$\Delta\rho_2 = |\mathbf{K_1}|/(16\pi^2 W), \qquad (2)$$

where $|\mathbf{K_1}|$, the momentum in the center-of-mass frame, and W are evaluated at bin center. We did not correct our data for radiative effects because explicit calculations showed that the radiative correction factors for the ΛK^+ and $n\pi^+$ channels agreed within $\pm 10\%$ for all bins [10], which is smaller than the systematic uncertainty of the

TABLE II. Sources and estimates of systematic uncertainties of the acceptance-corrected yields.

	Systematic Uncertainty		
Procedure	$n\pi^+$	$p\pi^0$	ΛK^+
Raw yield determination	**7%**	**17%**	**12%**
Hadron PID cuts	3%	10%	11%
Missing-mass cuts	3.5%	10.5%	2.5%
Background subtraction	5%	6%	0.3%
Efficiency correction	**6%**	**5%**	**5%**
Event generator dependence	1%	1%	0.7%
Fiducial cuts	2.5%	0.5%	0.2%
Trigger or tracking efficiency	5%	5%	5%
Phase space correction	**1.0%**	**0.4%**	**0.1%**
Total Uncertainty	**9%**	**18%**	**13%**

ratio, and showed no discernible kinematic dependence. Some corrected yields for the $p\pi^0$ channel were rejected for further analysis if the acceptance for the bin in question was lower than 2%.

The major sources and sizes of systematic uncertainties in the determination of the yields are summarized in Table II, grouped by category. Overall, we assign a systematic uncertainty of 9%, 18%, or 13% to the $n\pi^+$, $p\pi^0$, or ΛK^+ corrected yields, respectively.

We then fit the ϕ distributions of the corrected yields in each bin of Q^2, W, and $\cos\theta_m^*$ to the form $A + B\cos 2\phi + C\cos\phi$. Some fits were rejected in the case of the $p\pi^0$ channel if there were fewer than 9 ϕ data points (of a nominal 12) surviving the minimum acceptance cut. This procedure resulted in 60 independent fitted values of the (A) terms for the ΛK^+ and $n\pi^+$ channels, but only 48 for the $p\pi^0$ channel. We divided the (A) terms for the different channels to form the cross section ratios [11].

Figure 1 shows the three ratios of corrected yields plotted versus $\cos\theta_m^*$ with the different symbols representing different W bins. The two columns show the $\langle Q^2 \rangle = 1.9$ GeV^2 bin (left) and the $\langle Q^2 \rangle = 3.2$ GeV^2 bin (right). The shaded band is centered on the statistical average for each $\cos\theta_m^*$ bin with half-width equal to the systematic uncertainty on the ratio. Note that the three ratios are approximately the same for the two Q^2 bins while there is a noticeable falloff of the $\Lambda K^+/n\pi^+$ and $p\pi^0/n\pi^+$ ratios with $\cos\theta_m^*$. Figure 2 shows the same ratios as in Fig. 1, but plotted versus W. Again the two columns are for the two bins in Q^2. One can see that the ratios are approximately independent of W.

For purposes of comparing with the single value of λ_s used to characterize the ratio of strange to nonstrange hadronic production at high energy, we performed a weighted average over all bins for each ratio of final states, indicated by the flat dashed line. We obtain the following average values for the ratios: $\langle \Lambda K^+/n\pi^+ \rangle = 0.19 \pm 0.01 \pm 0.03$, $\langle p\pi^0/n\pi^+ \rangle = 0.43 \pm 0.01 \pm 0.09$, and
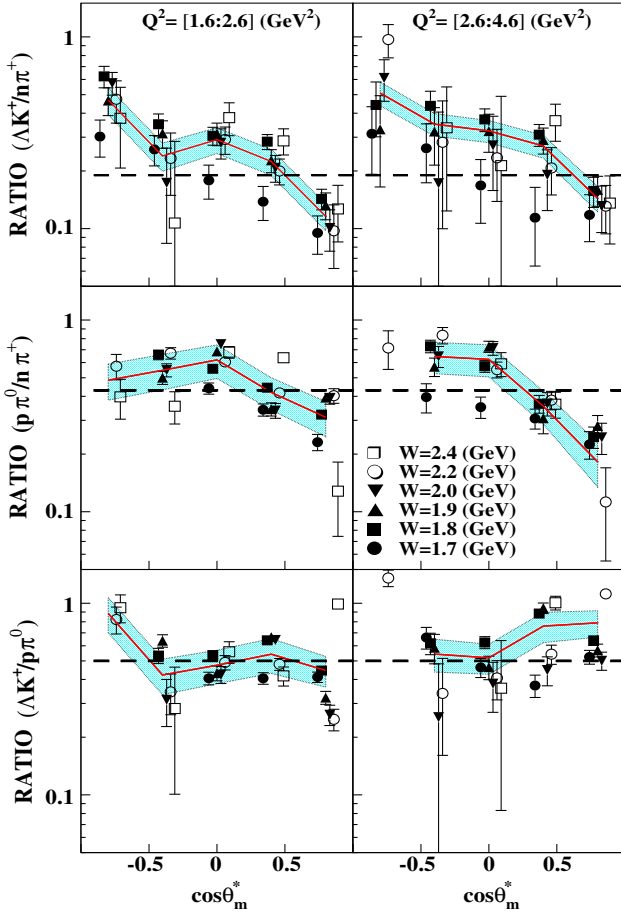
FIG. 1 (color online). Ratio of the three exclusive cross sections, ΛK^+ to $n\pi^+$ (top), $p\pi^0$ to $n\pi^+$ (middle), and ΛK^+ to $p\pi^0$ (bottom), for bins of $\langle Q^2 \rangle = 1.9$ GeV^2 (left) and $\langle Q^2 \rangle = 3.2$ GeV^2 (right), plotted versus $\cos\theta_m^*$ with different bins in W shown as different symbols. The systematic uncertainty is indicated by the shaded band, centered on the solid (red) line which connects the statistically weighted average for each bin. The flat dashed line represents the overall statistical average for each ratio. The data points are plotted slightly offset for clarity.

$\langle \Lambda K^+ / p\pi^0 \rangle = 0.50 \pm 0.02 \pm 0.12$; the first uncertainty is statistical and the second systematic.

We extracted the ratio of $q\bar{q}$ creation probabilities from these measured hadronic ratios using a simple factorization model in which a quark is knocked out of the proton followed by a single $q\bar{q}$ creation and appearance of the lightest baryon and pseudoscalar meson consistent with the quark flavor. We ignored other processes such as vector-meson coupling to the virtual photon or t-channel exchange, which might be responsible for the $\cos\theta_m^*$ dependence of our data. Nevertheless, we hope that the results from our simplified modeling are useful for comparison with strangeness suppression results from semi-inclusive production experiments analyzed under similar factorization assumptions. We note similarities of our model with that used by M. M. Kaskulov *et al.* [12] in
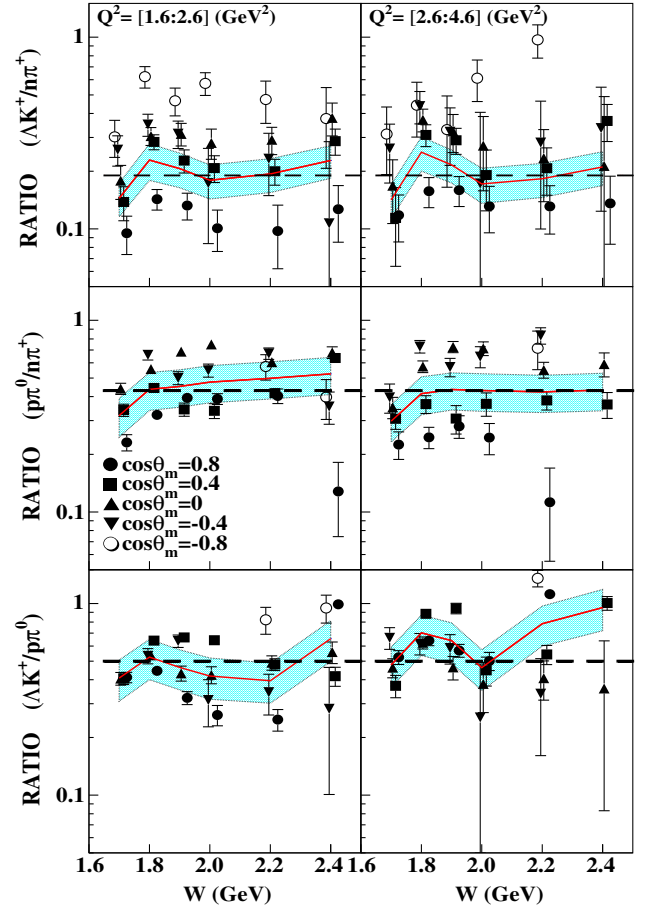
FIG. 2 (color online). Ratio of the three exclusive cross sections, displayed as in Fig. 1, but plotted versus W with different bins of $\cos\theta_m^*$ shown as different symbols.

fitting other data from Jefferson Lab on electroproduction of $n\pi^+$ from the proton.

In our model, events are initiated by virtual photon absorption by a valence u quark or d quark in the ratio of the sums of squares of the quark charges (8:1). This is followed by a single $q\bar{q}$ produced with probability $\mathbf{P}(q\bar{q})$, resulting in a $q\bar{q}$ state recoiling form a qqq state. Finally, the $q\bar{q}$ state hadronizes into the lowest energy meson state and the qqq state hadronizes into the lowest energy baryon state, in both cases with unit probability, resulting in three possible final states: $n\pi^+$, $p\pi^0$, or ΛK^+. Note also that we take into account that the π^0 is a 50:50 mixture of $u\bar{u}$ and $d\bar{d}$.

Following this simple arithmetic, the hadronic production rates ($\Re$) can be written in terms of the $q\bar{q}$ probabilities ($\mathbf{P}(q\bar{q})$) as such: $\Re(\Lambda K^+) \propto 8\mathbf{P}(s\bar{s})$, $\Re(n\pi^+) \propto 8\mathbf{P}(d\bar{d})$, and $\Re(p\pi^0) \propto 1/2(8\mathbf{P}(u\bar{u}) + 1\mathbf{P}(d\bar{d}))$.

We use the $\langle \Lambda K^+ / n\pi^+ \rangle$ ratio to solve for $s\bar{s}/d\bar{d}$ and the $\langle p\pi^0 / n\pi^+ \rangle$ ratio to solve for $u\bar{u}/d\bar{d}$:

$$s\bar{s}/d\bar{d} = \langle \Lambda K^+ / n\pi^+ \rangle = 0.19 \pm 0.01 \pm 0.03,$$
$$u\bar{u}/d\bar{d} = 2(\langle p\pi^0 / n\pi^+ \rangle - 1/16) = 0.74 \pm 0.02 \pm 0.18.$$

Finally, we use the $\langle \Lambda K^+/p\pi^0 \rangle$ ratio to determine an independent measure of the $s\bar{s}/d\bar{d}$ ratio. We obtain $s\bar{s}/d\bar{d} = 1/2(u\bar{u}/d\bar{d} + 1/8)\langle \Lambda K^+/p\pi^0 \rangle$, yielding

$$s\bar{s}/d\bar{d} = 0.28 \pm 0.01 \pm 0.07, \quad \text{assuming } u\bar{u}/d\bar{d} = 1.0, \text{ or}$$

$$s\bar{s}/d\bar{d} = 0.22 \pm 0.01 \pm 0.07, \quad \text{assuming } u\bar{u}/d\bar{d} = 0.74$$

$$\text{(as measured)}.$$

The systematic uncertainty on a $q\bar{q}$ ratio is simply that of the particle production ratio from which it is derived. We do not include factors due to the angular dependence of the ratios, nor do we attempt to quantify the systematic uncertainty of our hadronization model. Table III summarizes the results of this extraction.

We point out that our result of 0.74 ± 0.18 for the $u\bar{u}/d\bar{d}$ ratio is different from the value of unity expected from isospin invariance arguments, as assumed, for example, in high-energy hadronization models. However, we note that our hadron-production environment is explicitly not isospin invariant because the target is a proton, with two valence u quarks and one valence d quark. We speculate that the isospin dependence of our result for the $u\bar{u}/d\bar{d}$ ratio is related to the difference between the intrinsic $\bar{u}$ and $\bar{d}$ content of the proton as measured in Drell-Yan [13] and semi-inclusive DIS experiments [14]. Although intriguing, unfortunately our measurement is not significantly different from unity, especially when model uncertainties are included.

To summarize, our results show a sizable suppression of the ΛK^+ channel relative to the $n\pi^+$ and $p\pi^0$ channels from which we use a simple factorization model to estimate a strangeness suppression factor ($s\bar{s}/d\bar{d}$) of 0.19 ± 0.03, 0.22 ± 0.07, or 0.28 ± 0.07, depending on which data ratios we use and what we assume for the $u\bar{u}/d\bar{d}$ ratio. Interestingly, these values are similar to measurements of flavor suppression at high energies [3,5,6].

These determinations of the flavor dependence of $q\bar{q}$ creation are the first in the low-energy exclusive limit where the connection between the observed hadronic ratios and $q\bar{q}$ production probabilities is simple because only a single $q\bar{q}$ pair is created. However, further development of

exclusive reaction theory is needed to reduce the model dependence in the extraction of the $q\bar{q}$ creation probabilities from our data. We conclude by noting that understanding $q\bar{q}$ production dynamics is an important part of understanding color confinement in QCD and the fact that our values for strangeness suppression agree well with measurements done at much higher energy argues strongly for the universal nature of these dynamics.

[*]Corresponding author.
mestayer@jlab.org
[†]Present address: Old Dominion University, Norfolk, Virginia 23529, USA.
[‡]Present address: Universidad Técnica Federico Santa María, Casilla 110-V Valparaíso, Chile.
[§]Present address: Thomas Jefferson National Accelerator Facility, Newport News, Virginia 23606, USA.
[‖]Present address: University of Connecticut, Storrs, Connecticut 06269, USA.
[¶]Present address: Institut de Physique Nucléaire ORSAY, Orsay, France.
[**]Present address: University of Glasgow, Glasgow G12 8QQ, United Kingdom.

TABLE III. Values of ratio of $s\bar{s}$ to $d\bar{d}$ and $u\bar{u}$ to $d\bar{d}$ shown according to the experimental ratios from which they are derived. The "*a*" and "*b*" cases for the $\Lambda K^+/p\pi^0$ data set refer to the values of $u\bar{u}/d\bar{d}$ used in the extraction of the $s\bar{s}/d\bar{d}$ ratio: 0.74 for the "*a*" case and 1.0 for the "*b*" case. The uncertainties are the systematic uncertainties.

Ratio	$s\bar{s}/d\bar{d}$	$u\bar{u}/d\bar{d}$
$\Lambda K^+/n\pi^+$	0.19 ± 0.03	$\cdots$
$\Lambda K^+/p\pi^0$ "*a*"	0.22 ± 0.07	$\cdots$
$\Lambda K^+/p\pi^0$ "*b*"	0.28 ± 0.07	$\cdots$
$p\pi^0/n\pi^+$	$\cdots$	0.74 ± 0.18

[1] The phenomenology of color flux tubes which can "break" through the creation of $q\bar{q}$ pairs has a long history. Extending Schwinger's calculation, J. Schwinger, Phys. Rev. **82**, 664 (1951) of the vacuum production of e^+e^- pairs in an external electric field, the pioneering papers of L. Micu, Nucl. Phys. **B10**, 521 (1969); R. Carlitz and M. Kislinger, Phys. Rev. D **2**, 336 (1970) introduced the concept of $q\bar{q}$ vacuum pair creation; The binding force was approximated as a harmonic oscillator potential by A. Le Yaouanc, L. Oliver, O. Pène, and J. C. Raynal, Phys. Rev. D **8**, 2223 (1973); In 1979, A. Casher, H. Neuberger, and S. Nussinov, Phys. Rev. D **20**, 179 (1979); proposed a shorthand heuristic for describing the color flow between quarks, and Neuberger added finite time corrections in H. Neuberger, Phys. Rev. D **20**, 2936 (1979).

[2] B. Andersson, *The Lund Model* (Cambridge University Press, New York, 1998), as a modern overview.

[3] See results from the **UA1**, C. Bocquet *et al.*, Phys. Lett. B **366**, 447 (1996); **Jade**, W. Bartel *et al.*, Z. Phys. C **20**, 187 (1983); M. Althoff *et al.* (**Tasso** collaborations), Z. Phys. C **27**, 27 (1985); For a summary of earlier measurements of the strangeness suppression factor, see A. Wroblewski, Acta Phys. Pol. B **16**, 379 (1985); P. K. Malhotra and R. Orava, Z. Phys. C **17**, 85 (1983) and references therein.

[4] See http://home.thep.lu.se/~tobjorn/Pythia.html for general information on the "LUND-model" family of event generators.

[5] Results from the **OPAL**, G. Alexander *et al.* (**SLD** Collaborations), Phys. Lett. B **264**, 467 (1991); K. Abe *et al.*, Phys. Rev. D **59**, 052001 (1999).

[6] Results from the, F. D. Aaron *et al.* (**H1** Collaboration), Eur. Phys. J. C **61**, 185 (2009).

[7] P. Ambrozewicz *et al.*, Phys. Rev. C **75**, 045203 (2007).

[8] B. A. Mecking *et al.*, Nucl. Instrum. Methods Phys. Res., Sect. A **503**, 513 (2003).

[9] See, e.g., Eqs. (5)–(11) in W. R. Frazer, *Elementary Particles* (Prentice-Hall, Englewood Cliffs, 1966).

[10] K. Park, and M. D. Mestayer, CLAS Analysis Note Report No. 2013-103.

[11] The bin sizes and virtual photon flux factors are the same for the three channels and, thus, divide out in the ratio.

[12] M. M. Kaskulov, K. Gallmeister, and U. Mosel, Phys. Rev. D **78**, 114022 (2008).

[13] E. A. Hawker *et al.*, Phys. Rev. Lett. **80**, 3715 (1998).

[14] K. Ackerstaff *et al.*, Phys. Rev. Lett. **81**, 5519 (1998).